SYNTHESIS OF PbS AND Ni-DOPED PbS THIN FILMS BY CBD METHOD AND INVESTIGATION OF THEIR STRUCTURAL, OPTICAL AND PHOTOVOLTAIC PROPERTIES

S. HOROZ[a], A. EKINCI[b], O. SAHIN[c,*]

[a]*Department of Electrical and Electronics Engineering, Faculty of Engineering and Architecture, Siirt University, 56100 Siirt, Turkey*
[b]*Department of Nursing, School of Health, Siirt University, 56100 Siirt, Turkey*
[c]*Department of Chemical Engineering, Faculty of Engineering and Architecture, Siirt University, 56100 Siirt, Turkey*

In the first part of the present work, the structural, elemental and optical properties of PbS and PbS:Ni(3%) thin films synthesized by chemical bath deposition (CBD) technique on glass substrates at room temperature were analyzed by x-ray diffraction (XRD), energy dispersive x-ray (EDX) and absorption measurements, respectively. It was determined that the particle size of PbS:Ni (3%) thin film in the presence of Ni additive material is smaller than that of PbS although both thin films have the same structure (cubic phase). A similar result was achieved using the data obtained as a result of the optical measurements. Moreover, when the PbS thin film was doped with Ni, its energy band gap was observed to be wider. In the second part; the photovoltaic properties of FTO/Zn_2SnO_4/PbS and FTO/Zn_2SnO_4/PbS:Ni(3%) thin films were investigated by performing incident photon-to-current efficiency (IPCE) and current density (J)- voltage (V) measurements, respectively, using Zn_2SnO_4 coated on FTO conductive glasses instead of glass susbtrates. Based on the data obtained from both measurements, it was observed that the Ni dopant significantly enhance the performance of the PbS-based solar cell devices.

1. Introduction

Lead sulfide (PbS) commonly used in applications such as infrared sensors is one of the II-VI compound semiconductor group and has a narrow energy band gap of 0.4 eV [1-3]. Since PbS has large excitation Bohr radius, it is possible to see the quantum confinement effect for both electrons and holes in nano-sized PbS. Thus, the energy band gap of the PbS can be controlled by changing the particle size based on the effective mass model [4-5]. PbS semiconductor-based materials have received a great deal of attention in applications such as solar cells [4], photography [6] and ion-selective sensors [7]. Moreover, they have been used in different industrial technologies such as temperature sensors, diode lasers and decorative coatings [8-10].These properties are associated with PbS synthesis conditions. Therefore, different research groups have been able to synthesize such materials using different techniques such as chemical bath deposition [11], spray pyrolysis [12], microwave heating [13] and hydrothermal methods [14].

One of the most important factors affecting the optical properties of semiconductor materials is the doping of such semiconductors with metal ions.The doped metal ions result in a decrease in particle size and consequently an increase in the energy band gap [15-16]. In addition, the doping plays an active role in the use of semiconductor materials as promising sensitizers in solar cell applications owing to this feature. The observed increase in the energy band gap of a thin film in the nanocrystal structure may be related to the expected quantum confinement effect [17-19]. In the study by Castilla et al. [20], it was observed that the energy band gap of Ni and Cd-doped PbS thin films increase from 1.4 to 2.4 and 0.5 to 1.5 eV, respectively.Kumar et al. [21] and

---

[*]Corresponding author: omersahin@siirt.edu.tr

Das et al. [22] reported that the energy band gap of PbS thin films changed significantly when they were doped with Sb and Sn metals, respectively. Preetha et al. [23-24] emphasized in two different studies that the electrical conductivity of PbS thin films increases due to Al dopants when the They are doped with Al. In view of studies mentioned above, changes in the energy band gap of thin films doped with metal ions indicate that these materials can be used as sensitizers to improve performance in thin film based solar cell applications.

It is possible to synthesize semiconductor thin films by applying many different techniques. In previous different studies [11,25-26], PbS thin films have been synthesized by chemical bath deposition (CBD) method. One of the main reasons for using this technique is low cost. It was also emphasized that the desired PbS thin films were synthesized without the need for intensive laboratory conditions.

In the present study, structural, elemental and optical properties of PbS and PbS:Ni (3%) thin films synthesized by CBD method on glass substrates at room temperature were investigated. In addition to these properties, PbS and PbS:Ni(3%) thin films were synthesized on Zn_2SnO_4 coated on FTO conductive glasses to investigate the photovoltaic properties of PbS:Ni(3%) thin film in the presence of Ni dopant. Incident photon-to-current efficiency (IPCE) and current density (J)- voltage (V) measurements for PbS and PbS:Ni(3%) thin films were performed to calculate the power conversion efficiency value for both thin films.

2. Experimental part and characterizations

The materials required to synthesize PbS and PbS:Ni(3%) thin films by CBD method are lead nitrate ($Pb(NO_3)_2$), thioacetamide (C_2H_5NS), nickel nitrate hexahydrate ($Ni(NO_3)_2.6H_2O$), sodium hydroxide (NaOH) and triethanolamine (TEA) ($C_6H_{15}NO_3$), respectively.0.1 M $Pb(NO_3)_2$, 0.1 M C_2H_5NS, 0.5 M NaOH and a certain amount of TEA were mixed in an 80 mL beaker to synthesize PbS thin film on a glass substrate at room temperature.The stirring process was continued until a homogeneous solution was obtained.Then a thoroughly cleaned glass substrate was immersed in the solution in a vertical position.The glass substrate was left in the PbS solution for approximately 3 hours, then removed, washed several times with distilled water, and air dried.To synthesize the PbS: Ni (3%) thin film on a glass substrate with the same method, 0.003 M $Ni(NO_3)_2.6H_2O$ was added to the above-mentioned solution and then all the steps were repeated.For IPCE and J-V measurements, Zn_2SnO_4 coated on FTO conductive glasses by doctor blade methode was used as substrate instead of glass substrates.

X-ray diffraction (XRD) in a Rigaku x-ray diffractometer with Cu Kα (λ = 154.059 pm) radiation was used to characterize the structural properties of thin films. UV-VIS absorption spectra were recorded using a Perkin-Elmer Lambda 2 spectrometer. Energy dispersive x-ray (EDX) (JEOL JSM 5800) was used to study the elemental analysis of PbS and PbS:Ni(3%) thin films. The IPCE and J-V measurements were carried out using PCE-S20 with a monochromatic light source consisting of a 150 W Xe lamp and a monochromator.

3. Results and discussions

The diffraction patterns obtained from XRD measurements for PbS and PbS:Ni(3%) thin films are shown in Fig. 1(a-b).

a) PbS

b) PbS:Ni(3%)
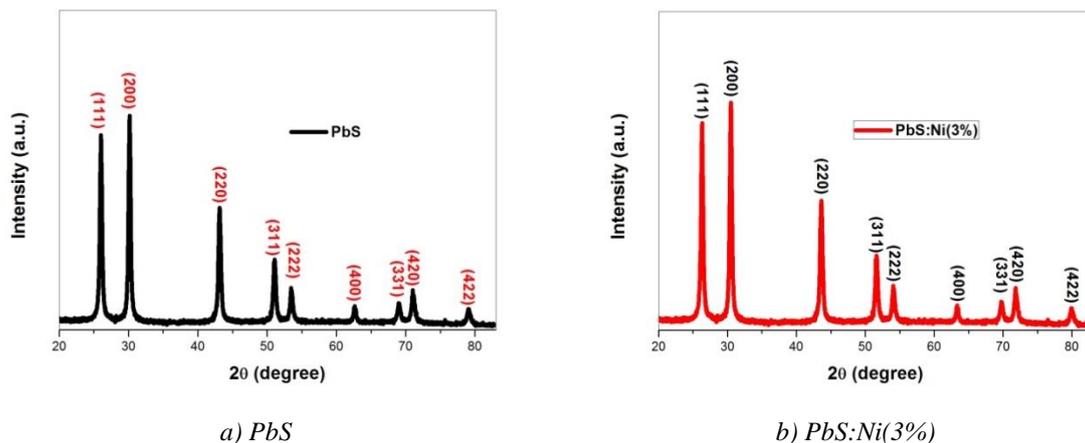
Fig. 1 XRD patterns for PbS and PbS:Ni thin film synthesized by CBD technique at room temperature.

(111), (200), (220), (311), (222), (400), (311), (420) and (422) were observed and it was determined that the two thin films shows a cubic structure using the XRD reference database of PbS. In the XRD data of the PbS:Ni(3%) thin film shown in Fig. 1b, no extra diffraction pattern that may be caused by undesired Ni compounds is observed, which can be regarded as an indication that this thin film is successfully synthesized at the desired level.

The calculated lattice constants (α) of PbS and PbS:Ni(3%) thin films using the equation given in Equation (1) for the (111) plane are shown in Table 1.

$$\alpha = \frac{\lambda}{2sin\theta}\sqrt{h^2 + k^2 + l^2} \tag{1}$$

The terms shown in Equation (1) are: α: lattice constant, λ = wavelength of XRD, (hkl): Miller indices, θ: Bragg's angle.

Table 1. Calculated α value for PbS and PbS:Ni(3%) thin films synthesized by CBD technique at room temperature.

Samples (thin films)	2θ value at (111) plane (degree)	Calculated α value (nm)
PbS	26.00	0.592
PbS:Ni(3%)	26.23	0.586

Based on the data shown in Table 1, the results obtained are that (1) there is a shift in the diffraction pattern corresponding to the (111) plane of PbS:Ni(3%) thin film, (2) The α value of PbS:Ni(3%) thin film is lower than that of pure PbS. The reason for the observed decrease in α value may be that Ni dopant is easily incorporated into PbS:Ni(3%) thin film since the ionic radius of Ni^{2+}(0.069 nm) is smaller than the ionic radius of Pb^{2+}(0.119 nm).

The average particle sizes (*t*) of the thin films synthesized by the CBD technique were calculated using the Debye-Schreer relation given in Ref. [27], taking into account the diffraction patterns corresponding to (111), (200) and (220) planes demonstrated in Fig. 1 (a-b). The *t* values calculated using full width at half maximum (FWHM) are shown in Table 2.

Table 2. Calculation average particle size for thin films using the Debye-Schreer equation synthesized by CBD technique at room temperature.

Samples (thin film)	FWHM (radyan)	t (nm)
PbS	0.00609	25.97
PbS:Ni(3%)	0.00661	23.91

As can be seen in Table 2, it is concluded that PbS:Ni(3%) has larger FHWM and smaller t-value than pure PbS thin film. Thus, although the structure of the thin film is not changed when PbS thin film is doped with Ni, its size decreases compared to pure PbS. In other words, it can be said that the Ni additive influences the PbS thin film size.

Elemental properties of PbS:Ni(3%) thin film was investigated by energy dispersive x-ray (EDX) measurement. The EDX spectra of thin film is shown in Fig. 2. As is cleraly seen from Fig. 2, observation of the spectrum of Ni element is another indication that PbS:Ni (3%) thin film is efficiently synthesized. Using the EDX spectrum, the real concentration (%) of Ni in PbS:Ni (3%) thin film was determined as approximately 1.70. It is thought that the loss of Ni in PbS:Ni(3%) thin film could be owing to the wash process during synthesis.
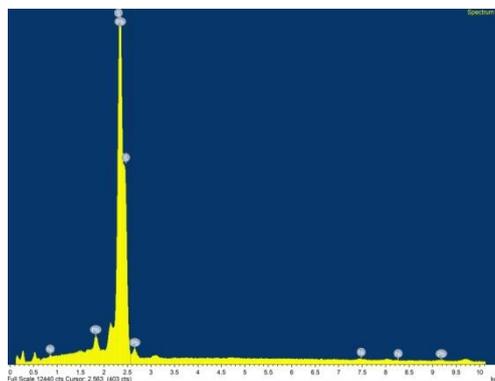
Fig. 2. EDX spectrums of PbS:Ni(3%) thin films synthesized by CBD technique at room temperature.

Optical absorption measurements were carried out to examine the optical properties of thin films and to determine their energy band gap. The absorption spectra for PbS and PbS:Ni(3%) thin films are shown in Fig. 3a-b as a result of optical measurements using UV-Vis absoption spectroscopy.

a) PbS
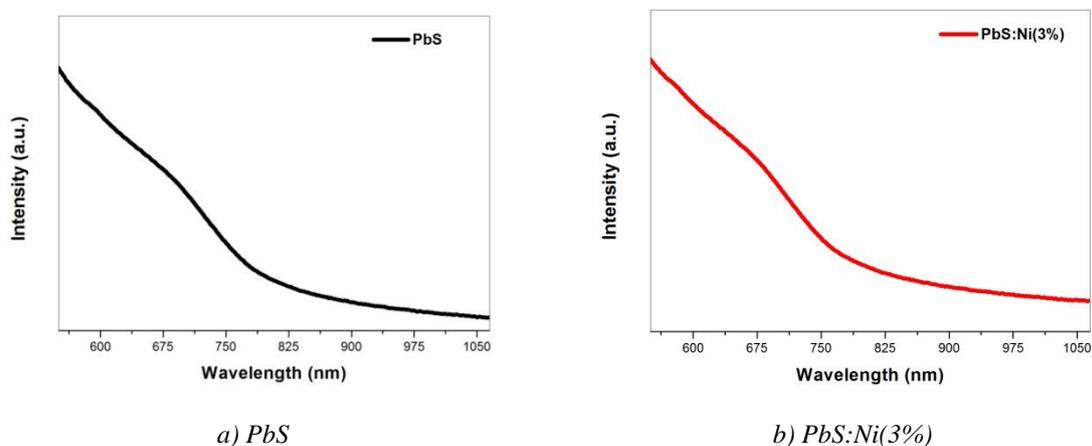
b) PbS:Ni(3%)

Fig. 3 Optical absorption spectra for PbS and PbS:Ni(3%) thin film synthesized by CBD technique at room temperature.

Based on the data shown in Fig. 3 a-b, graphs of $(\alpha h\nu)^2$ versus hν, indicated in Fig. 4 a-b, were obtained using the Tauc relation is given in Ref. [28].

a) PbS   *b) PbS:Ni(3%)*
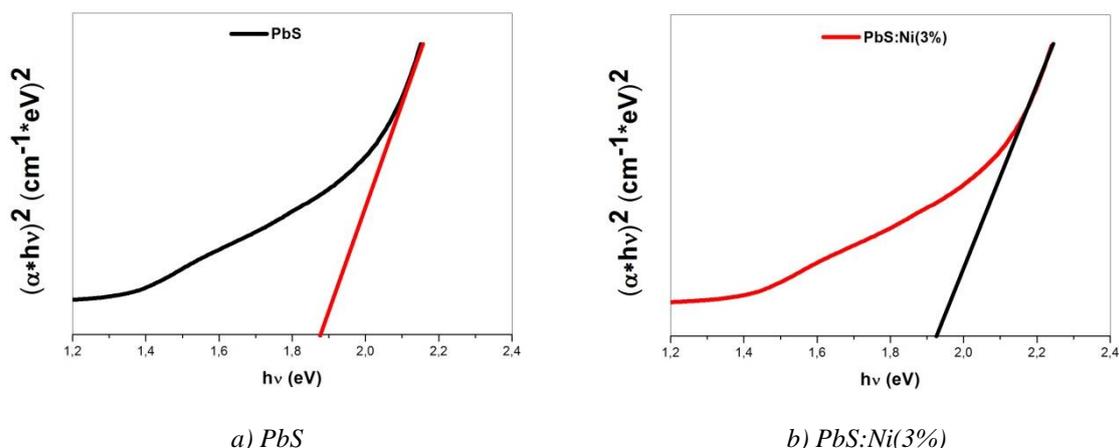
Fig. 4 Graphs of $(\alpha h\nu)^2$ versus hν for PbS and PbS:Ni(3%) thin film synthesized by CBD technique at room temperature.

Here, α is absorption coefficient, his Plank's constant and ν is the frequency. Thus, the energy band gap values obtained for PbS and PbS:Ni(3%) thin films are 1.89 and 1.94 eV, respectively. Clearly, the value of PbS:Ni(3%) thin film is higher than that of PbS. This result is an indication that the energy band gap to PbS changes when PbS is doped with Ni. From the perspective of optical absorption spectra, it can be seen that the absorption wavelength (~639.2 nm) of PbS:Ni (3%) thin film is shifting to the shorter wavelength compared to pure PbS (~656.1 nm). This phenomenon, called blue shift, can be explained by the quantum confinement effect. This effect occurs if crystal size of the synthesized material is equal to or less than its exciton radius. Another meaning of the quantum confinement effect is that as the particle size of thin films decreases, the energy band gap value of that thin film increases.

Another process using the energy band gap valueis to determine the crystal sizes of PbS and PbS:Ni(3%) thin films using the Brus's formula [29], which is shown in Equation (2).

$$E_{thin\,film} = E_{bulk} + \frac{h^2}{8r^2}\left(\frac{1}{m_e^*} + \frac{1}{m_h^*}\right) \tag{2}$$

The terms shown in Equation (2) are: $E_{thin\,film}$: energy band gap value (eV) of synthesized semiconductor thin film, E_{bulk}:energy band gap value (eV) of semiconductor bulk, h: Plank's constant, r: size (nm) of thin film, m_e^*: effective mass of electron, m_h^*:effective mass of hole. The size values obtained as a result of the calculation are shown in Table 3.

Table 3. Calculation size for PbS and PbS:Ni(3%) thin filmsynthesized by CBD technique at room temperature.

Samples (thin film)	Energy band gap values (eV)	Particles sizes (nm)
PbS	1.89	22.85
PbS:Ni(3%)	1.94	22.19

It was found that Nidopant results in the reduction in size of PbS:Ni(3%) thin film which clearly relates with increasing in the band gap value. Thus, it was observed that the particle sizes calculated for thin films as a result of the optical measurements and the particle sizes obtained using the XRD measurements are in agreement with each other.

IPCE measurements were performed to investigate the photovoltaic properties of PbS and PbS:Ni(3%) thin films synthesized on Zn_2SnO_4 coated on FTO conductive glasses by CBD technique at room temperature. The IPCE spectra recorded as a result of the measurements are demonstrated in Fig. 5a-b.
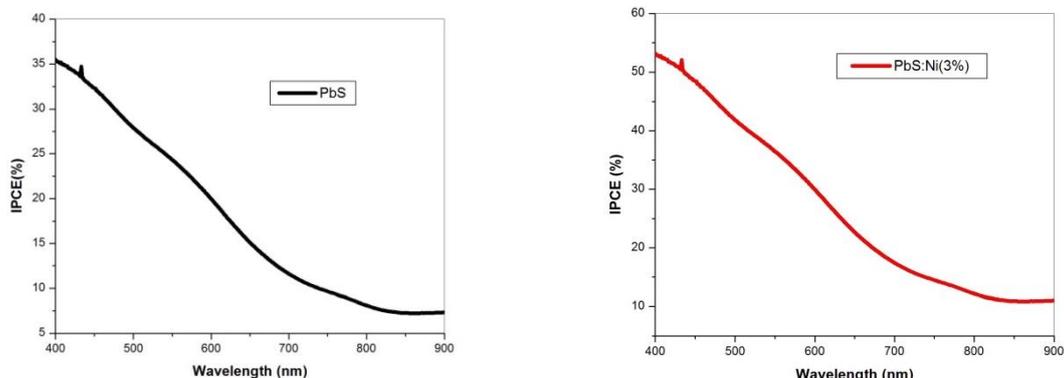
a) FTO/Zn₂SnO₄/PbS   b) FTO/Zn₂SnO₄/PbS:Ni(3%)

Fig. 5 Recorded IPCE spectra for FTO/Zn₂SnO₄/PbS and FTO/Zn₂SnO₄/PbS:Ni(3%)
thin film synthesized by CBD technique at room temperature.

Whereas the value of IPCE (%) obtained for undoped PbS thin film at approximately 400 nm is 35, it is seen that this value is increased up to 50% for PbS:Ni(3%). Thus, it can be said that the photovoltaic property of PbS:Ni(3%) thin film has improved due to Ni additive material. Another effect due to the presence of Ni additive is that the spectral response of PbS:Ni(3%) thin film is wider than that of PbS. In this case, the formation of dark current is suppressed.

Another process for studying photovoltaic properties is to obtain the J-V curves of thin films. Power conversion efficiency (η) values of thin films were calculated using the obtained curves. The J-V curves for PbS and PbS:Ni(3%) thin films synthesized on Zn_2SnO_4 coated on FTO conductive glassesby CBD technique at room temperature are indicated in Fig. 6a-b.
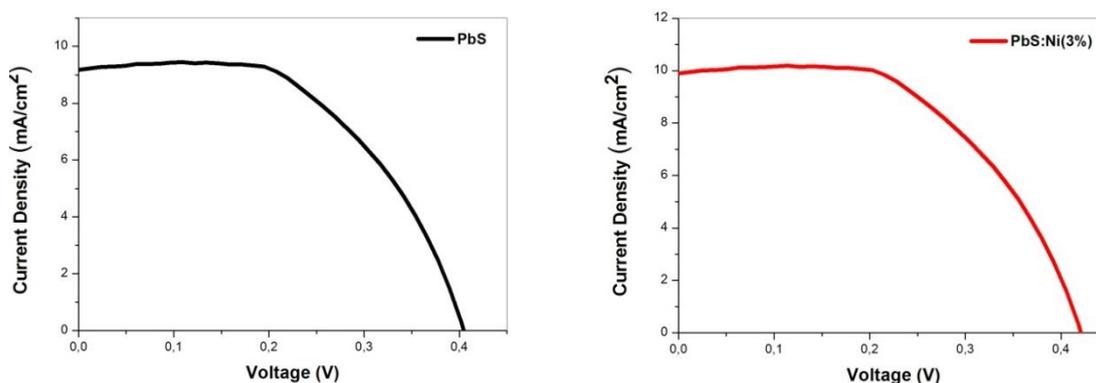
a) FTO/Zn₂SnO₄/PbS   b) FTO/Zn₂SnO₄/PbS:Ni(3%)

Fig. 6a. Recorded J-V curves for FTO/Zn₂SnO₄/PbS and FTO/Zn₂SnO₄/PbS:Ni(3%) thin film
synthesized by CBD technique at room temperature.

Table 3 shows the ηvalues calculated for both thin films using V_{OC} and J_{SC} values determined from the curves shown in Fig. 6.

Table 3. Values of V_{OC}, J_{SC} and η (%) for FTO/Zn$_2$SnO$_4$/PbS and FTO/Zn$_2$SnO$_4$/PbS:Ni(3%) thin filmssynthesized by CBD technique at room temperature.

Samples (thin film)	V_{OC} (V)	J_{SC} (mA/cm^2)	η (%)
FTO/Zn$_2$SnO$_4$/PbS	0.40	9.22	2.02
FTO/Zn$_2$SnO$_4$/PbS:Ni(3%)	0,42	10.01	2.27

Taking into account the calculated performance values, Ni dopant seems to be an important factor to boost the efficiency of PbS-based solar cells.Thus, both IPCE and J-V measurements have been shown experimentally that Ni-doped PbS thin films can be used as promising sensitizers in photovoltaic applications.

4. Conclusions

In the first part of the present study, PbS and PbS:Ni(3%) thin films were successfully synthesized on glass substrate by CBD technique at room temperature. Structural, elemental and optical properties of thin films grown on glass substrates were investigated. It was observed that the structure of both thin films is cubic. It was also determined that the particle size of PbS:Ni(3%) thin film is smaller than PbS using the obtained XRD patterns. In other words, the Ni dopant affects the particle size while not altering the structure of PbS. Since PbS:Ni(3%) thin film has a smaller particle size, it is expected that energy band gap of PbS:Ni(3%) thin film is wider than that of PbS. the expectation was confirmed as a result of the optical measurements made. Thus, the energy band gap for PbS and PbS:Ni(3%) thin films was determined as 1.94 and 1.88 eV, respectively.

In the second part of the study, IPCE and J-V measurements were performed to investigate the photovoltaic properties of PbS and PbS:Ni(3%) thin films. Thin films were synthesized on Zn$_2$SnO$_4$ coated on FTO conductive glasses by the same technique at room temperature for the application of these measurements. The obtained IPCE(%) values at 450 nm for PbS and PbS:Ni(3%) thin films are 35 and 50, respectively. Using the J-V curves, the calculated η (%) values for PbS and PbS:Ni(3%) thin films are 2.02 and 2.27, respectively. Based on the data obtained from both measurements, it was observed that the Ni dopant significantly enhance the performance of the PbS-based solar cell devices.

References

[1] R. S. Mane, C.D. Lokhande, Materials Chemistry and Physics **65**, 1 (2000).
[2] C. Rajashree, A. R. Balu, Optik- International Journal for Light and Electron Optics **127**, 8892 (2016).
[3] N. V. Le, H. T. Nguyen, H. V. Le, T. T. P. Nguyen, Journal of Electronic Materials **46**, 274 (2017).
[4] E. Veena, K. V. Bangera, G. K. Shivakumar, Applied Physics A **123**, 366 (2017).
[5] A. S. Obaid, M. A. Mahdi, Z. Hassan, M. Bouaydina, Materials Science in Semiconductor Processing **15**, 564 (2012).
[6] P. K. Nair, O. Gomezdaza, M. T. S. Nair, Advanced Functional Materials **1**, 139 (1992).
[7] Y. G. Vlasov, E. A. Buchkov, Sensors and Actuators **12**, 275 (1987).
[8] S. T. Navala, D. K. Bandgar, M. A. Chougule, V. B. Patil, RSC Advances **5**, 6518 (2015).
[9] J. J. Peterson, T. D. Krauss, Nano Letters **6**, 510 (2006).
[10] C. Rajashree, A. R. Balu, V. S. Nagarethinam, Journal of Materials Science: Materials in Electronics **27**, 5070 (2016).
[11] A. J. Perez, C. A. M. Perez, E. C. dela C. Terrazos, M. A. Q. Lopez, Materials Letters **121**, 19

208

(2014).

[12] M. G. Faraj, M. Z. Pakhuruddin, International Journal of thin Films Science and Technology, **4**, 215 (2015).

[13] M. Sabet, M. S. Niasari, Electrochimica Acta **169**, 168 (2015).

[14] M. Kord, K. Hedayati, M. Farhadi, Main Group Metal Chemistry **40**, 35 (2017).

[15] S. Horoz, Q. Dai, F. S. Maloney, B. Yakami, J. M. Pikal, X. Zhang, J. Wang, W. Wang, J. Tang, Physical Review Applied **3**, 024011 (2015).

[16] S. Horoz, Superlattices and Microstructures **111**, 1043 (2017).

[17] J. Wang, Q. Shen, T. Izuishi, Z. Pan, K. Zhao, X. Zhang, Journal of Materials Chemistry A. **4**, 877 (2016).

[18] H. J. Kim, H. D. Lee, C. S. S. P. Kumar, S. S. Rao, S. H. Chung, D. Punnoose, New Journal of Chemistry **39**, 4805 (2015).

[19] G. Rimal, A. K. Pimachev, A. J. Yost, U. Poudyal, S. Maloney, W. Wang, T. Chien, Y. Dahnovsky, J. Tang, Applied Physics Letters **109**, 103901 (2016).

[20] S. R. Castilla, M. Z. Totatzintle, R. B. L. Flores, L. C. Lima, O. P. Moreno, Journal of Materials Science Engineering A **3**, 305 (2013).

[21] R. Kumar, R. Das, M. Gupta, V. Ganesan, Superlattices and Microstructures **75**, 601 (2014).

[22] R. Das, R. Kumar, Materials Research Bulletin **47**, 239 (2012).

[23] K. C. Preetha, T. L. Remadevi, Physica B. **407**, 4173 (2012).

[24] K. C. Preetha, T. L. Remadevi, Materials Science Semiconductor Processing **24**, 179 (2014).

[25] E. Yucel, Y. Yucel, Ceramics International **43**, 407 (2017).

[26] A. N. Fouda, M. Marzook, H. M. A. El-Khalek, S. Ahmed, E. A. Eid, A. B. El-Basaty, Silicon **9**, 809 (2017).

[27] S. Horoz, L. Lu, Q. Dai, J. Chen, B. Yakami, J. M. Pikal, W. Wang, J. Tang, Applied Physics Letters **101**, 223902 (2012).

[28] Z. Q. Mamiyev, N. O. Balayeva, Optical Materials **46**, 522 (2015).

[29] C. Cheng, J. Li, X. Cheng, Journal of Luminescence **188**, 252 (2017).